Theor. Appl. Climatol. (2007)
DOI 10.1007/s00704-007-0318-0
Printed in The Netherlands

Theoretical and Applied Climatology

[1] Department of Environmental Sciences, University of Virginia, Charlottesville, VA, USA
[2] Department of Atmospheric Science, University of Wyoming, Laramie, WY, USA
[3] Department of Physics, Howard University, Washington, DC, USA

Vertical attributes of precipitation systems in West Africa and adjacent Atlantic Ocean

J. D. Fuentes[1], B. Geerts[2], T. Dejene[1], P. D'Odorico[1], and **E. Joseph[3]**

With 9 Figures

Received October 23, 2006; revised February 22, 2007; accepted March 7, 2007
Published online July 9, 2007

Summary

This study reports the findings of TRMM (Tropical Rainfall Measuring Mission) satellite data analyses undertaken to investigate differences in intensity and depth of precipitating systems in the transition region from continental to maritime environments in West Africa during the rainy season of June to September in 1998–2004. The results of this study are interpreted in the context of regional thermodynamic variables such as equivalent potential temperature and equivalent convective available potential energy to discern the processes governing storm development. Over continental West Africa, convective-type precipitating storms exhibit a substantially larger vertical extent compared to the ones over the eastern Atlantic Ocean. In contrast, the stratiform precipitating systems show similar vertical reflectivity patterns, depth and intensity over both land and adjacent ocean in West Africa. The differences in the attributes of storms, as they move from the continent to the ocean, can be partly explained in terms of the surface-atmosphere interactions that provide the necessary transports of energy and water vapor from the surface to the cloud layer.

1. Introduction

Much of the rainfall over West Africa and adjacent Atlantic Ocean is the result of organized convection. The characteristics of West Africa mesoscale convective systems (MCSs) have been studied using geostationary satellites (Hodges and Thorncroft, 1997; Diedhiou et al., 1999) and radars during field campaigns such as the GARP (Global Atmospheric Research Program) Atlantic Tropical Experiment (GATE), (Reed, 1977; Houze and Betts, 1981). Based on these and limited field work (e.g. Roux, 1988), it is now established that most of the rainfall in West Africa is associated with linear or more amorphous MCSs whose spatial extent can reach 500 km (Lebel et al., 2003). Typical MSCs tend to last 12 h (unless they become Cape Verde tropical cyclones) and some squall lines can persist for 2 days (Laing and Fritsch, 1997; Redelsperger et al., 2002). Mesoscale organized convection is often associated with the African Easterly Jet and tends to occur in regions of synoptic-scale low-level convergence (Cook, 1999; Lebel et al., 2003). In general, substantial atmospheric instability due to warm, moisture-rich boundary-layer air, and strong low-level vertical wind shear are the necessary conditions to sustain the propagation of squall lines in West Africa (Rotunno et al., 1988; Rowell and Milford, 1993; Weisman and Rotunno, 2004). Over the West African land area, MSCs move faster due to the stronger African Easterly Jet and have shorter lifetimes compared to the ones over the east Atlantic Ocean (Hodges and Thorncroft, 1997).

Despite the extensive research carried out over West Africa during the last four decades, limited knowledge still exists on the dynamics, thermodynamics, and microphysical characteristics of precipitating storms as they migrate from continental to maritime environments.

The launching of the TRMM (Tropical Rainfall Measuring Mission) satellite during 1997 started a new era of space borne precipitation research (Simpson et al., 1988). With the TRMM data it is now possible to investigate the vertical attributes of precipitation systems using reflectivity profiles derived from the Precipitation Radar (PR) aboard the satellite (Kummerow et al., 2000; Kozu et al., 2001). TRMM-derived vertical profiles of precipitation and hydrometeors indicate in which layers of the atmosphere diabatic heating occurs (Lin et al., 2004; Schumacher et al., 2004). Knowledge of the vertical distribution of diabatic heating is crucial to establish the energy balance of the tropical atmosphere. The TRMM PR products also allow establishing a distinction between convective or stratiform rainfall (Schumacher and Houze, 2003). Such distinction is important because of the resulting different relationships between radar reflectivity, Z, and rain rates, R (Z–R relationships), that can be defined for the estimation of spatial rainfall (Steiner and Houze, 1997). The Z is expressed in the units of $\mathrm{mm}^6\,\mathrm{m}^{-3}$. For practical purposes, in this study and elsewhere the decibel (dB) units are used because of the large range in Z values. Z can be interpreted as a range-independent measure of radar backscatter intensity. If all scatterers are spherical drops too small to reach the Mie scattering regime (about 3 mm in diameter for the case of the PR) then Z equals the integral of the 6^{th} power of the droplet diameter, D. In practice, Z is an equivalent reflectivity. R is the rain rate at the level of the Z measurement, although it is often applied at the surface. Because Z is proportional to the 6^{th} power of D and R is proportional to the 3–4^{th} power of D, the Z–R relationships are not necessarily exact. Nevertheless radars are widely used, even in space, with the primary purpose of estimating rain rates.

Utilizing TRMM data, the attributes of convection and precipitation-type designation (Houze, 1997) in remote regions such as the Congo Basin in central Africa and the Amazon region in South America can be studied. For instance, compared to the Amazon region, the Congo Basin experiences deeper storms with higher reflectivity values above the freezing level (e.g. at 7 km), higher fraction of convective-type rainfall, stronger 85-GHz ice scattering signature, and more lightning activity (Boccippio et al., 2000; Petersen and Rutledge, 2001; Toracinta et al., 2002; Sealy et al., 2003; Geerts and Dejene, 2005; Petersen et al., 2006; Schumacher and Houze, 2006). The identified storm attributes indicate that precipitation systems over the Congo Basin exhibit characteristics of tropical continental convection whereas those over the Amazon show similar aspects of maritime convection (Cecil and Zipser, 2002; Toracinta et al., 2002; Nesbitt and Zipser, 2003). In essence, the term maritime refers to the characteristic rain drop size distribution, which in turn is governed by the number of cloud condensation nuclei. Several studies (Stith et al., 2002; Williams et al., 2002) have documented Amazonian cloud droplet spectra similar to those observed over maritime environments, especially during easterly flow regimes (Halverson et al., 2002). The fundamental reason of the difference between Amazonian and Congo storms is that the low-level Easterly Trade winds proceed unimpeded from the Atlantic into the Amazon whereas the access of these winds into the Congo Basin is blocked by the elevated terrain of East Africa.

Several TRMM-PR-based studies have focused on sub-Saharan Africa. For example, Adeyewa and Nakamura (2003) showed that the TRMM-PR climatological rainfall patterns in Africa exhibit a significant difference, compared to rain gauges and other satellite-derived rainfall estimates. This difference is seasonally- and regionally-dependent and it is smallest in the wet season of the northern savanna region. Nicholson et al. (2003) performed a similar comparison, and found that the TRMM PR rainfall tends to exceed rain gauge rainfall in West Africa. Given this uncertainty, Geerts and Dejene (2005) did not examine the TRMM-PR surface rainfall, and instead studied the vertical features of precipitating systems over Africa as inferred from the TRMM PR data. They found that in all African regions, but especially in the Sahel and northern savannas, storms exhibit high echo tops, high hydrometeor loading aloft, and a low-level evaporation signature. Also, their work revealed a strong diurnal modulation of storms in the Sahel and northern savannas where they are most common around sunset.

Schumacher and Houze (2006) recently investigated stratiform-precipitation production over sub-Saharan Africa and the eastern Atlantic Ocean. They showed that the east Atlantic Ocean has more rainfall arising from shallow storms, while sub-Saharan Africa experiences more non-precipitating anvils. In an investigation of the temporal variability of precipitation in sub-Saharan Africa, Mohr (2004) concluded that the diurnal rainfall cycle is strongly influenced by organized convection.

The thermodynamics and microphysical characteristics of storms in West Africa and eastern Atlantic Ocean remain poorly understood. The TRMM data sets provide a unique opportunity to investigate the spatial and temporal characteristics of storms over a region of the world where ground-based rainfall measurements remain sparse. Therefore, the main goal of the present study is to investigate differences in radar reflectivity of precipitating storms in both West Africa and downstream maritime environments. Seven years of TRMM PR data are used for the rainy season (June–September). The results of this study are interpreted in the context of regional thermodynamic variables such as equivalent potential temperature and ''equivalent'' convective available potential energy ($CAPE_e$) as these variables exert influences on storm development. In previous studies (Geerts and Dejene, 2005), a methodology was developed for binning individual TRMM PR precipitation profiles in terms of time of day, region, and criteria such as season and surface rain rates. The emphasis of earlier studies was to identify the vertical features of storms and associated diurnal precipitation variability in several regions of Africa. The present investigation adopts a similar methodology as that included in Geerts and Dejene (2005) but focuses on different regions in West Africa to consider the climatological attributes of storms in the zonal belt stretching from sub-Sahara Africa to the adjacent Atlantic Ocean.

2. Research methodology

2.1 Data sources

The data included in this study came from two sources. The TRMM data are one source. Before August 2001 the TRMM satellite orbited at an altitude of about 350 km above mean sea level. After August 2001 the satellite orbiting altitude became 403 km above mean sea level. The satellite carries a 13.8-GHz precipitation radar (PR), the multi-frequency TRMM imager (TMI), the Visible and Infrared Scanner (VIRS), the lightning imaging sensor (LIS), and the clouds and Earth's radiant energy system (CERES) (Kummerow et al., 1998). Since December 1997, measurements made with the TRMM radar and passive microwave radiometer are providing uninterrupted data sets of rainfall rate and vertical attributes of precipitating systems. The TRMM satellite follows a non-Sun-synchronous orbit, specifically designed such that at any location all times of the day have a roughly equal overpass chance. Thus, a sufficiently long composite of TRMM data will represent the full diurnal cycle and will enable studies of the diurnal variability of precipitation. The PR range resolution is 250 m. Thus, for zenith beams the vertical resolution of the reflectivity profile is 250 m. However, at high ($>15^\circ$) inclination angles the vertical resolution decreases to 1000 m due to the relatively large footprint size (Heymsfield et al., 2000). Because the low inclination angles allow for a higher resolution in the vertical profile, only measurements made at inclinations of $\pm 12^\circ$ from nadir were included in the analyses presented here. Before the TRMM satellite was boosted to a new orbiting altitude, the horizontal resolution of the PR was about 4.3 km at nadir and about 5 km at the maximum inclination of 17° (Kummerow et al., 1998). After the TRMM satellite was boosted, the horizontal resolution at nadir became 5 km. The above-mentioned uncertainty in surface rainfall applies to both ends of the rain rate spectrum. At the low end, the limited horizontal and low radar sensitivity (17 dBZ) prevent the observation of isolated and small (<5 km in diameter) storm cells (Heymsfield et al., 2000). This limitation can introduce an underestimate of surface rainfall by as much as 25%, mostly in regions outside of deep convection (Sauvageot et al., 1999). However, an improvement of surface rainfall estimates has resulted from the implementation of a correction for the effect of non-uniform beam filling (Durden et al., 1998). The PR-based reflectivity profiles included in the present study were corrected for attenuation by heavy rain using the surface reference technique (Iguchi and

Meneghini, 1994). The TRMM 2A25-volumetric radar reflectivities, surface rain rates (Iguchi et al., 2000), and rain type (Awaka et al., 1997), and the TRMM PR 3B42 monthly-mean surface rain rate are the primary datasets used in this study.

The second source of information was the National Center for Environmental Prediction (NCEP)–National Center for Atmospheric Research (NCAR) global re-analysis data set (Kalnay et al., 1996). Thermodynamic variables were determined from the NCEP reanalysis to aid with the interpretation of TRMM data analyses and the associated results included in the present study.

2.2 Data processing

Seven years (from 1998 to 2004) of data were included to derive vertical profiles of reflectivity over West Africa and the eastern Atlantic Ocean (Fig. 1) during the course of the rainy season corresponding to the months of June to September. The full vertical resolution of the 2A25 PR (250 m) data was considered as this study focused on the reflectivity profile of precipitating systems. The 3-hour temporal resolution was chosen to capture the diurnal variation in rainfall, while maintaining statistical significance by using a relatively large sample size. Here the temporal resolution relates to the data bin size. The choice of temporal resolution was based on the results reported by Negri et al. (2002). Based on 3 years of TRMM data they concluded that, because of spatially inconsistent sampling, the 1-hour temporal resolution is inadequate to describe the diurnal cycle of precipitation. More recently, Hirose et al. (2007) determined that the currently available 8 years of TRMM data allow a depiction of the diurnal cycle of precipitation at 1-hour resolution in areas as small as $0.2^\circ \times 0.2^\circ$ blocks ($\sim 20 \times 20\,\mathrm{km}^2$). This is more optimistic than Negri et al. (2002), who used only 3 years of data. Given that the blocks used here are larger than $20 \times 20\,\mathrm{km}^2$, our results are statistically robust. The relatively large region (Fig. 1) selected for this study permitted the use of a 3-hour temporal sampling to adequately capture important features in the diurnal variability of precipitating systems. The results are reported in local solar time.

To study changes in the characteristics of precipitating storms along a zonal transect from continental West Africa to the Atlantic Ocean, differences in reflectivity profiles were investigated for the following three regions, from east to west (Fig. 1): I) Continental West Africa (5° W–20° E), II) coastal West Africa (17.2–5° W), and III) eastern Atlantic Ocean (25.0–17.2° W). These regions share a common meridional extent (4.5–17.5° N). This study focuses on east-west variations. Most of the rainfall, and thus most of the reflectivity profiles in this study, occur in a narrow belt between 6 and 10° N (Fig. 1), corresponding to the belt of most frequent wet-season MCSs and highest sea surface temperature offshore, ranging between 27 and 28 °C (Fontaine and Janicot, 1996). This regional classification was mainly based on the expected distinct attributes

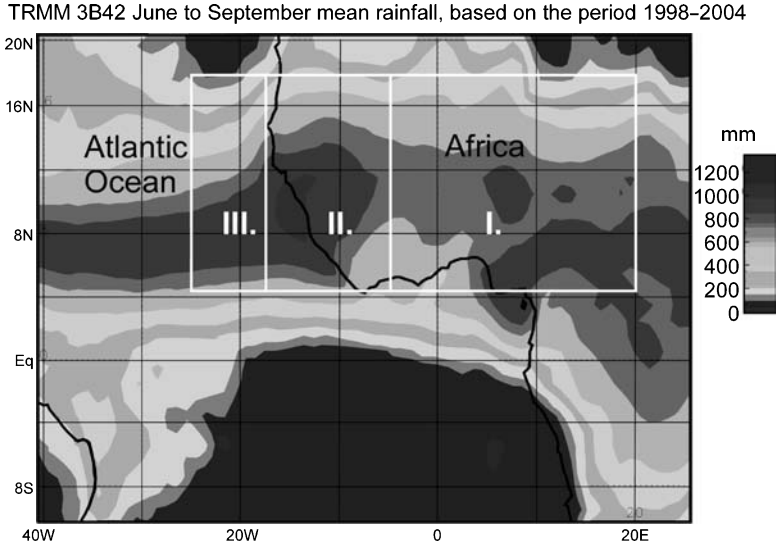

Fig. 1. Map of West Africa illustrating the three regions (marked with the boxes) established for the present study. The shaded contours represent the average precipitation patterns (in mm) estimated for the months of June to September during 1998–2004 using TRMM 3B42

of storms associated with easterly waves that move from the continent to the ocean (Reed, 1977). Figure 1 shows the spatially average rainfall patterns estimated for the months of June to September during 1998–2004 using TRMM 3B42 data.

The frequency distribution of the TRMM PR reflectivity as a function of altitude was estimated for the available satellite data in each region. The estimated frequency distribution for a given reflectivity, Z, at a certain altitude, z, was normalized in such a manner that the sum of all frequencies amounted to 100% (Yuter and Houze, 1995). In each region, the estimated frequency distribution was grouped into stratiform and convective regimes based on the rain data type designation of the 2A25 TRMM data algorithm (version 6). Here we will contrast characteristic storm intensity and depth for both convective and stratiform regimes.

Following Geerts and Dejene (2005), several indices were defined to identify differences in vertical storm characteristics for the regions considered in the present study. The evaporative index (EI) was defined to evaluate the differences in the potential rates of low-level evaporation of rainfall. The EI was estimated as the difference in reflectivity between the altitudes of 4.0 km, the highest level unambiguously below the radar bright band (Battan, 1973), and 2.0 km. To identify the presence of the bright band and determine the decay of reflectivity above the bright band, the stratiform index (SI) was defined as the difference in reflectivity between the altitudes of 7.0 and 4.5 km. Both EI and SI were estimated for individual reflectivity profiles and were expressed in dBZ units. Reflectivity values below the PR threshold sensitivity (17 dBZ) were not included in the EI and SI calculations. Also, the hydrometeor precipitable water (HPW) was estimated as the integral of water content in the atmospheric column from the surface to the top of the atmosphere (1).

$$\mathrm{HPW} = \frac{1}{\rho_1}\int_0^{\mathrm{Top}} \rho(z)q(z)\ \mathrm{d}z \tag{1}$$

ρ_1 and $\rho(z)$ are water and air density (kg m^{-3}), respectively. The vertical distribution of water vapor mixing ratio (g kg^{-1}), $q(z)$, was estimated based on reported algorithms (Battan, 1973) relating reflectivity (Z) to $q(z)$, applicable to summertime precipitation (in North America). The units of HPW are depth (m or mm) of the water column. From the surface to 4.5 km, where rain is assumed to occur, $q(z)$ was estimated using (2a). Relationship (2b) was considered in the $q(z)$ calculations for altitudes greater than 4.5 km, where snow is assumed to occur.

$$q(z) = 0.0032\,Z^{0.55}\exp\left(\frac{z}{8}\right) \tag{2a}$$

$$q(z) = 0.0068\,Z^{0.45}\exp\left(\frac{z}{8}\right) \tag{2b}$$

In (2) z represents altitude (in km) and Z is the reflectivity (expressed in mm^6 m^{-3}, in dB units, dBZ). Additionally, to discern the precipitation efficiency (Hobbs et al., 1980) of the storms for the identified three regions, the storm productivity index (SPI, units of hour^{-1}) was defined as the ratio of the surface rain rate (in mm per hour) over the HPW generated by a given storm.

To examine thermodynamic differences among the storms in the identified regions, the NCEP–NCAR re-analysis data were used to interpret the main observations deduced from the 2A25 TRMM data. For each region, $\mathrm{CAPE_e}$ (in J kg^{-1}) was estimated for the months of June to September, based on profiles of monthly-mean temperature and humidity. The $\mathrm{CAPE_e}$ values were estimated using relationship (3) (Petersen and Rutledge, 2001).

$$\mathrm{CAPE_e} = R_\mathrm{d}\int_{\mathrm{LFC_e}}^{\mathrm{LNB_e}} (\theta_\mathrm{e}^* - \theta_{\mathrm{e,sfc}})\mathrm{dlnp} \tag{3}$$

$\mathrm{LFC_e}$ is the level of free convection, $\mathrm{LNB_e}$ is the level of neutral buoyancy, θ_e is the equivalent potential temperature. θ_e^* and $\theta_{\mathrm{e,sfc}}$ are the saturation equivalent potential temperature and the surface equivalent potential temperature, respectively. The variable p is the pressure (in Pascal) and $\mathrm{R_d}$ is the specific gas constant for dry air (287 J kg^{-1} K^{-1}). Positive parcel buoyancy occurs at levels where $\theta_{\mathrm{e,sfc}}$ exceeds the local θ_{e^*} (i.e. between $\mathrm{LNB_e}$ and $\mathrm{LFC_e}$, Petersen and Rutledge, 2001).

3. Results and discussion

3.1 Diurnal variability in the characteristics of precipitating storms

In West Africa and adjoining areas of eastern Atlantic Ocean strong convection occurs during

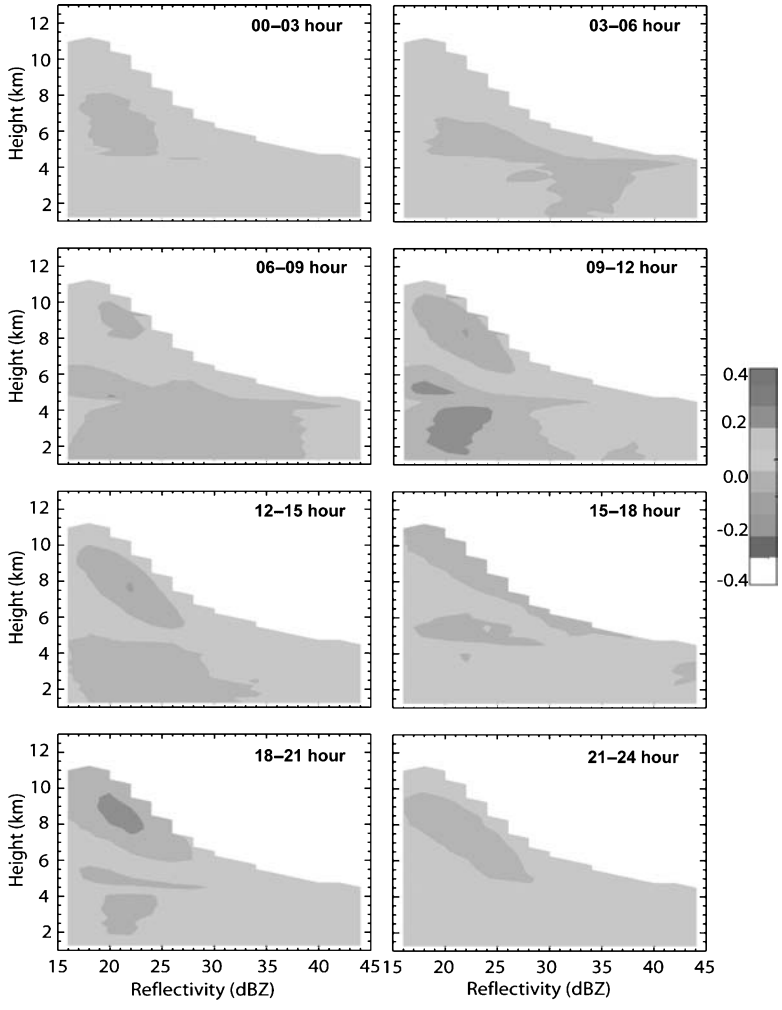

Fig. 2. Diurnal variation of frequency distribution of reflectivity for continental West Africa [units $(2\,\mathrm{dBZ})^{-1}$ $(250\,\mathrm{m})^{-1}$]. The normalized frequencies are expressed as a difference from the normalized 24 h mean values. The bar on the right hand side of the figure provides the scale for the estimated frequencies

the months of June to September, especially along the latitudinal belt of the Inter-tropical Convergence Zone (ITCZ) (Fontaine and Janicot, 1996). The dynamics of precipitating systems are locally invigorated by diurnally varying surface energy fluxes and lower tropospheric wind shear. The horizontal and vertical extent of the identified storms and their duration varied depending on factors such as proximity to the moisture sources, heat capacity of the location, and presence of the African Easterly Jet. Thus, to investigate the evolution of precipitating systems in the transition region from continental West Africa to eastern Atlantic Ocean, we first analyzed the diurnal variability of the vertical attributes of precipitating storms over the three study regions. A diurnal delay (relative to local solar noon) in the vertical radar reflectivity of the identified storms was evident in all three regions (Figs. 2, 3 and 4). A time lag in the changes of the reflectivity profile was observed along the transect going from continental to oceanic regions. Strong and deep echoes occurred mostly during 15–21 h (local time, LT) over continental West Africa (Fig. 2). Over coastal West Africa, the maximum reflectivity values took place during 18–24 LT (Fig. 3). On the other hand, over the eastern Atlantic Ocean, the diurnal precipitation cycle had a smaller amplitude and deep echoes occurred mostly during 06-12 LT (Fig. 4). The peaks in the low-level (shallow) convection also showed a time lag from continental West Africa to eastern Atlantic Ocean. Shallow convection was most frequent during 9–12 LT, 12–15 LT and 15–18 LT over continental West Africa, coastal West Africa and eastern Atlantic Ocean, respectively. The deeper storms over continental and coastal West Africa were most likely triggered by daytime surface heating and water vapor transport over the continental regions. In the summer, water vapor advection from

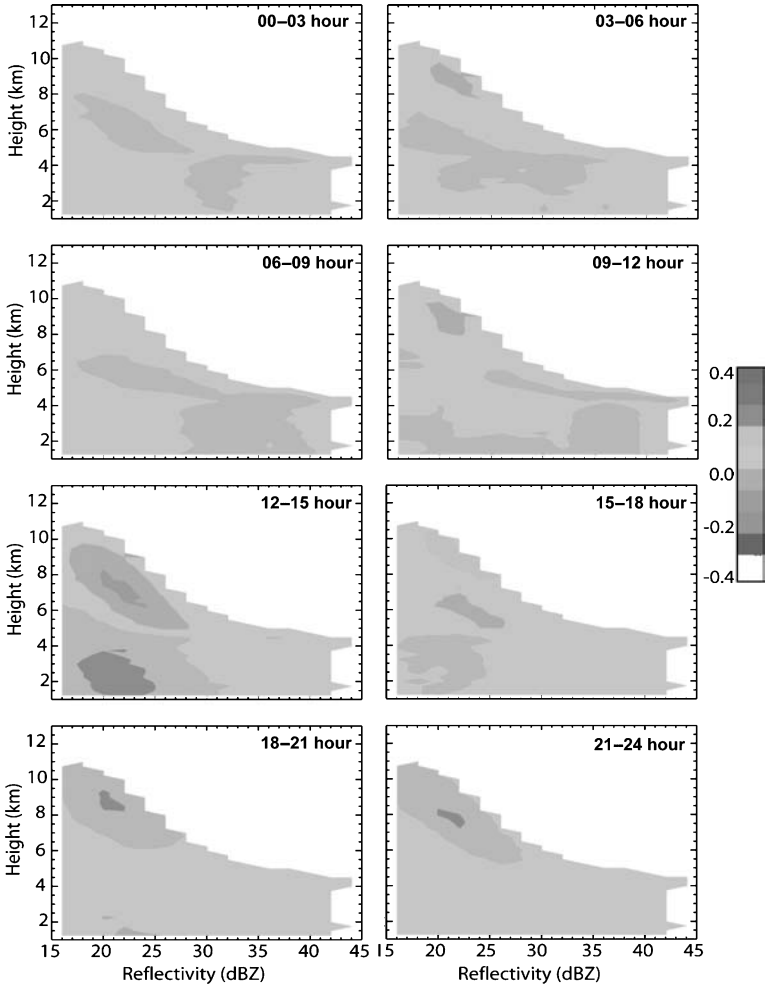

Fig. 3. As Fig. 2, but for coastal West Africa

the south peaks at night in West Africa (Cook, 1999; Paeth and Friederichs, 2004). Additionally, there might be distinct differences in the cloud microphysical properties between the continental and maritime atmospheres of West Africa. Over the continental areas terrigenous materials may provide the necessary cloud condensation nuclei. In contrast, over the central Atlantic Ocean sea-salt aerosols and dust act as the principal nucleation agents. The early morning maximum of deep echoes over the ocean (Fig. 4) is consistent with results from previous studies (Geerts and Dejene, 2005; Schumacher and Houze, 2006). Offshore MCSs often form near midnight and reach their maximum intensity in the morning (Hodges and Thorncroft, 1997). Furthermore, the present results suggest that storm systems that develop over coastal West Africa in the evening period are frequently sustained by the favorable nocturnal marine environment after exiting the coast.

3.2 Regional variability of the vertical storm characteristics

Regional differences in the vertical structure of precipitating storms were evident along the established transect from the continental region of West Africa to the eastern Atlantic Ocean. For stratiform-type precipitation, the frequency distribution for all regions exhibited similar patterns (Fig. 5), and the average reflectivity profiles in stratiform precipitation were remarkably similar in the three regions (Fig. 6). Schumacher and Houze (2006) also found similar patterns in the same region during a different time period. A signature of stratiform precipitation is the presence of a bright band which was observed at an altitude of about 4.5 km in all three regions (Fig. 6). Compared to continental West Africa, echo tops were about 1 km lower over the eastern Atlantic Ocean. Additionally, the isolines below the freezing level were shifted to lower reflectivities for

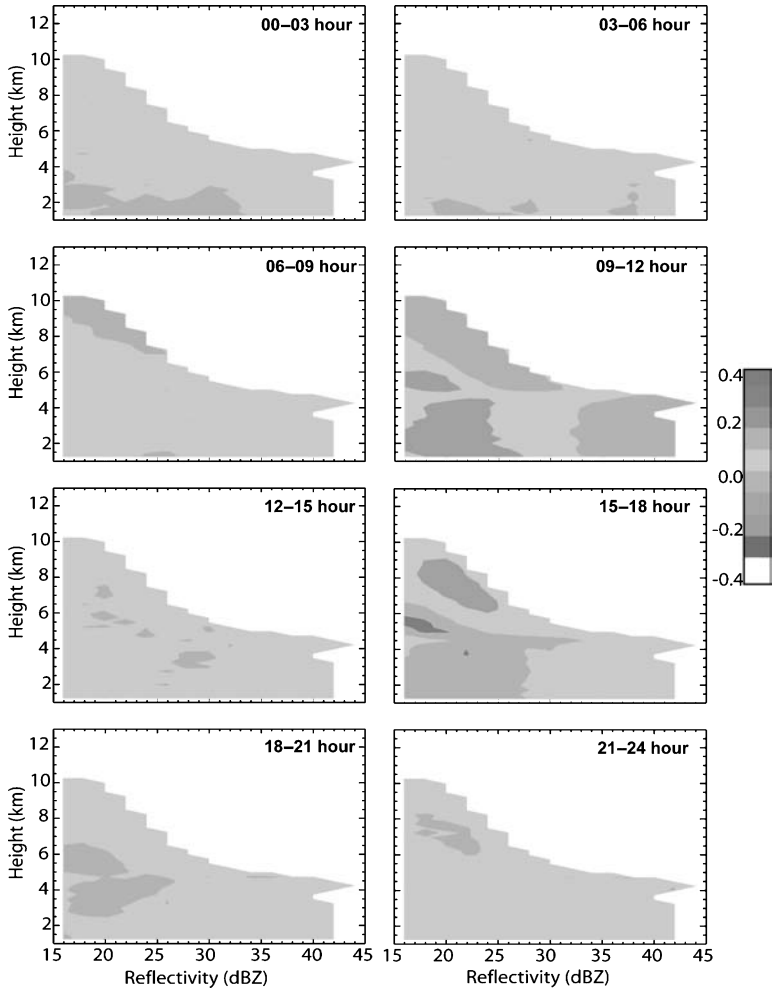

Fig. 4. As Fig. 2, but for eastern Atlantic Ocean

the stratiform-type precipitation over continental West Africa, suggesting low-level evaporation over the region (Hirose and Nakamura, 2004; Geerts and Dejene, 2005). Low-level evaporation was deduced from the more frequent occurrence of higher reflectivities near the 4-km level as compared to closer to the ground. The angle of tilt was systematic such that it was almost vertical (with no much tilt) for coastal West Africa and the tilt to higher reflectivities significantly increased for eastern Atlantic Ocean, indicating low-level raindrop growth or dominance of warm rain processes over the region.

Convective storms became less deep and less intense over the ocean (Figs. 5 and 6). The implication is that maritime convection had a lower hydrometeor content above the freezing level than continental storms in West Africa. The reflectivity frequency occurrences of convective storms over the three regions (Fig. 5) show that shallow convection progressively became more common from continental West Africa to the eastern Atlantic Ocean, consistent with the TRMM-PR study reported by Schumacher and Houze (2006). The high frequency occurrence of reflectivities ranging from 20 to 30 dBZ at low elevation suggested that light convective rain, for instance from cumulus congestus, was relatively common over the eastern Atlantic Ocean. As a result, the mean reflectivity profile for oceanic convection exhibited lower values compared to that over the adjacent continent (Fig. 6). In order to further define and contrast the vertical variations of reflectivity, the mean profile and the frequency distribution for reflectivities exceeding certain threshold levels (i.e. 17, 27, and 37 dBZ) were determined (Fig. 7). The mean profiles were calculated by taking the mean of all reflectivities (in Z units) for each level. Note that the reflectivity profiles present the probabilities, varying with height, that at least a certain reflectivity value (exceeding 17, 27, or 37 dBZ) can be found

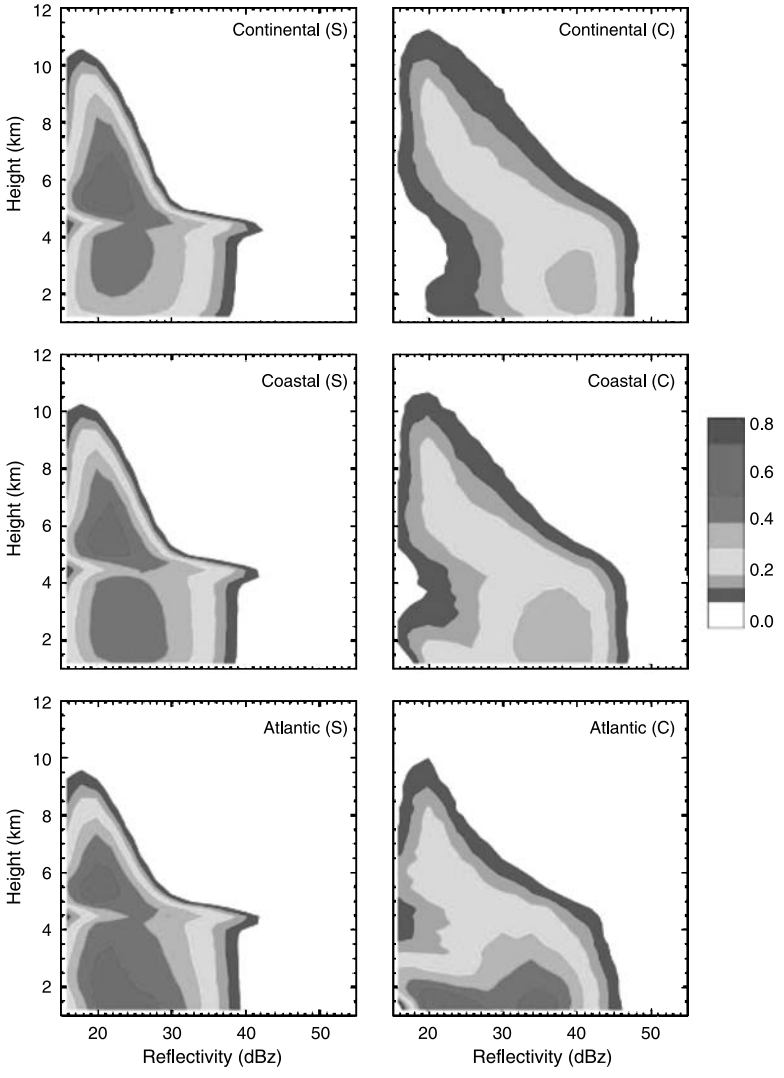

Fig. 5. Ensemble probability density functions estimated based on the relationship of reflectivity as a function of altitude for the regions identified in Fig. 1. The left and right panels of figures report result for stratiform (S)- and convective (C)-type precipitation, respectively, during June to September (1998–2004). The results are based on the TRMM 2A25 data (1998–2004). The bar on the right hand side of the figure provides the scale for the estimated probabilities

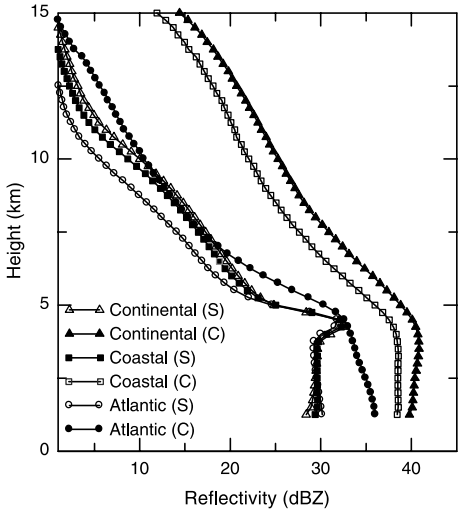

Fig. 6. Ensemble average reflectivity as a function of altitude for the regions identified in Fig. 1 during June to September (1998–2004)

when it rains on the ground (the 17 dBZ threshold includes all measurable intensities of precipitation, 27 dBZ includes moderate and heavy precipitation, and 37 dBZ includes only heavy precipitation; the profiles depict the typical vertical structure of precipitating systems). The frequency of the lowest reflectivity threshold at low levels was much greater over the eastern Atlantic Ocean, and the rapid decay of this threshold with height indicates that many systems were shallow. The echo frequency over continental West Africa decreased towards the ground for all threshold reflectivity levels, suggesting evaporation or breakup of raindrops (Fig. 7). In contrast, the echo frequency (reflectivity count) over coastal West Africa and eastern Atlantic Ocean increased from just below the freezing level down to near the ground. This indicated that raindrops grow as they

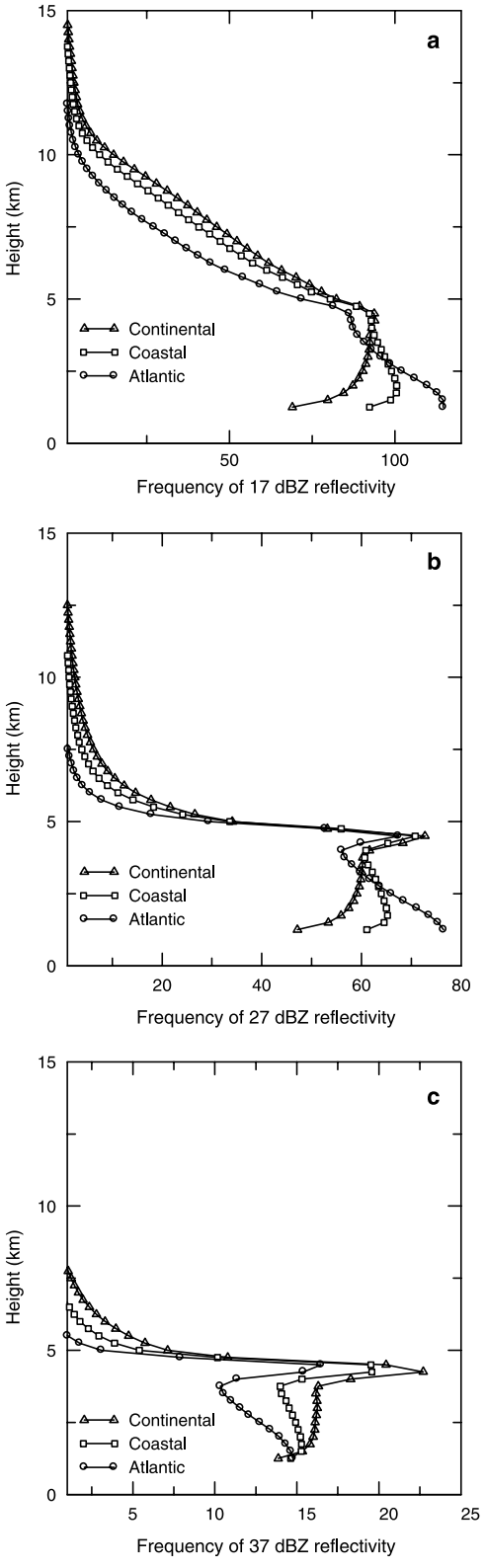

Fig. 7. Frequency distribution of reflectivity values plotted against altitude. Three thresholds reflectivity values chosen for the analyses included (**a**) 17, (**b**) 27 and (**c**) 37 dBZ. The frequencies were normalized by the number of rain profiles in each region

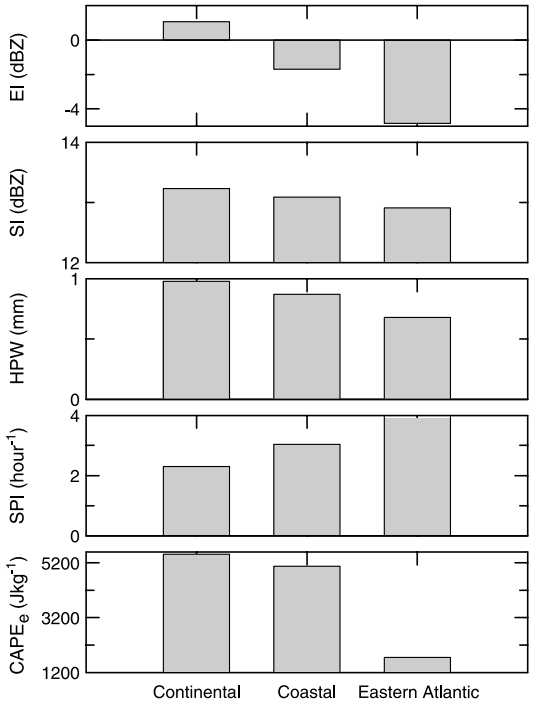

Fig. 8. Average values of the indices estimated to define the characteristics of precipitating systems in West Africa. The SI is the evaporation index (in dBZ), SI is the stratiform index (in dBZ), HPW is the hydrometeor precipitable water (in mm), and $CAPE_e$ is the equivalent convective available energy (in $J\,kg^{-1}$)

move towards ground, implying a dominance of warm-rain processes and low-level cloud base over the eastern Atlantic Ocean.

Key differences were also revealed in various precipitation indices estimated for the three regions (Fig. 8). Precipitation systems over continental West Africa had the higher evaporative index (EI) compared with the east Atlantic Ocean, indicating higher evaporation of water drops before reaching the ground. The EI decreased substantially along the land-to-ocean transect, with the lowest value over the eastern Atlantic Ocean. The negative EI there is likely due to the low-level growth of raindrops by the collision-coalescence process. The stratiform signature (SI) was high in all regions with less regional variability, suggesting that a high proportion of stratiform precipitation exists in all the regions. Continental West Africa tended to have deeper storms with higher HPW, and therefore also had a low SPI value (i.e. a relatively high water volume aloft for a given surface rain rate). On the other hand, storms over the eastern Atlantic Ocean were more efficient rain producers (higher SPI) due

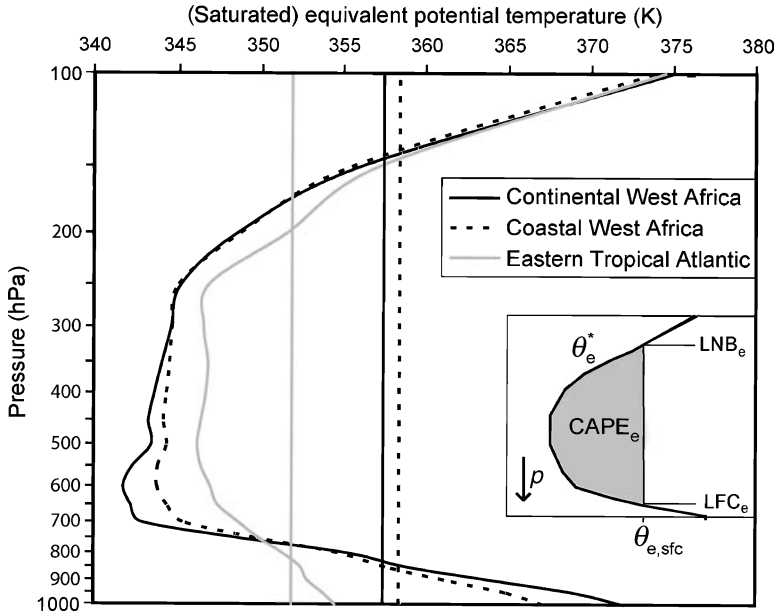

Fig. 9. Vertical profiles of θ_e^* (curved lines) plotted as a function of pressure (log coordinate) for various regions. The vertical lines are corresponding values of θ_e derived from the temperature and specific humidity at 1000 hPa. Data are based on NCEP–NCAR re-analysis data

to lower HPW associated with shallow precipitating systems.

The highest $CAPE_e$ values were estimated for the continental West Africa, followed closely by coastal West Africa (Fig. 9). On average, the eastern Atlantic Ocean had much lower $CAPE_e$ values. The differences in the CAPE values are mostly associated with the higher values of LNB_e for continental and coastal West Africa. The continental and coastal West Africa regions had higher LNB_e levels (150 hPa) than for the eastern Atlantic Ocean (200 hPa). These $CAPE_e$ results are consistent with the more frequent occurrences of PR echoes recorded at the upper levels in those regions (Figs. 5 and 7). In general, the relatively weaker storms and higher warm-rain fraction over the eastern Atlantic Ocean were consistent with the lower values of $CAPE_e$ compared with the continental and coastal West Africa.

4. Discussion and conclusions

This study described the regional and diurnal variability of the vertical attributes of precipitating systems along the continental-maritime transition region in West Africa. The diurnal peak in maximum vertical storm structure occurred between 15 and 21 LT in continental West Africa, and 12–15 h later over the eastern Atlantic Ocean. Shallow convection over these regions also showed a westward time lag, peaking at 9–12 LT, 12–15 LT and 15–18 LT over continental West Africa, coastal West Africa and eastern Atlantic Ocean, respectively.

In West Africa, organized convection generally moves westward. From the TRMM data source it is not clear whether the MSCs, peaking in the evening over land, were the same as those observed into the early morning over water. However, such offshore storm travel has been previously documented (Hodges and Thorncroft, 1997). Convective storms exhibited different attributes along the investigated land-to-ocean transect. For example, in the eastern Atlantic Ocean storms were shallower and had lower integrated hydrometeor content (Fig. 8). This difference applies mostly to those parts of storms classified as convective. Over continental West Africa, the stratiform precipitation did not differ much from those over the adjacent ocean (Fig. 5).

Furthermore, the echo strength from 4 km down to the ground increased for the eastern Atlantic Ocean and decreased for continental West Africa (Fig. 6). These profiles can be explained by low-level evaporation and/or raindrop break-up over continental West Africa as opposed to low-level drop size growth over the eastern Atlantic Ocean due to a much lower cloud base there. The higher cloud base, more intense low-level evaporation, and deeper convection observed over the continent likely result from surface-atmosphere interactions, specifically the high sensible heat fluxes over land. Over land, such interactions affect the surface energy and moisture balance with a con-

sequent impact on the availability of energy to enhance convection. In addition, the occurrence of raindrop break-up, as suggested by the decrease in echo-frequency towards the ground, may be caused by the differences in cloud condensation processes resulting from the different aerosol types prevailing over land and ocean (e.g. Williams et al., 2002). Warm-rain processes likely dominated over the eastern Atlantic Ocean as a result of the growth or increase in hydrometeor content at low elevation. The frequency isolines of reflectivity below the freezing level tilted to lower reflectivity values over continental West Africa, indicating a low proportion of shallow precipitation clouds, and/or low-level evaporation. The isolines gradually tilted to higher reflectivity values towards the surface from coastal to eastern Atlantic Ocean, suggesting low-level rain drop growth. Over the eastern Atlantic Ocean purely warm rain clouds were more likely to occur than over land (Fig. 5).

The intensity and depth of convective storms systematically decreased from continental West Africa to the eastern Atlantic Ocean. The regional changes in the vertical characteristics of precipitating storms, observed using the TRMM PR 2A25 data, are consistent with the changes in $CAPE_e$ of the basic environment estimated from NCEP–NCAR re-analysis data.

Acknowledgments

TRMM is a project cosponsored by NASA and NASDA, the Japanese space agency. This research was supported by NASA grant NAG5-13778. Courtney Schumacher of Texas A&M University provided excellent suggestions to improve the manuscript. Two reviewers are thanked for providing comments that considerably improved the quality of the manuscript.

References

Adeyewa ZD, Nakamura K (2003) Validation of TRMM radar rainfall data over major climatic regions in Africa. J Appl Meteor 42: 331–347

Awaka J, Iguchi T, Kumagai H, Okamoto K (1997) Rain type classification algorithm for TRMM Precipitation Radar. Proc. of the IEEE 1997 Intl. Geoscience and Remote Sensing Sym., Aug. 3–8, Singapore, pp 1633–1635

Battan LJ (1973) Radar observations of the atmosphere. University of Chicago Press, 324 pp

Boccippio DJ, Goodman SJ, Heckman S (2000) Regional differences in tropical lightning distributions. J Appl Meteor 39: 2231–2248

Cecil DJ, Zipser EJ (2002) Reflectivity, ice scattering, and lightning characteristics of hurricane eyewalls and rainbands. Part II: Intercomparison of observations. Mon Wea Rev 130: 785–801

Cook K (1999) Generation of the African Easterly Jet and its role in determining West African precipitation. J Climate 12: 1165–1184

Diedhiou A, Janicot S, Viltard A, de Felice P, Laurent H (1999) Easterly wave regimes and associated convection over West Africa and tropical Atlantic: results from the NCEP/NCAR and ECMWF reanalyses. Clim Dynam 15: 795–822

Durden SL, Haddad ZS, Kitiyakara A, Li FK (1998) Effects of non-uniform beam filling on rainfall retrieval for the TRMM precipitation radar. J Atmos Oceanic Technol 15: 635–646

Fontaine B, Janicot S (1996) Sea surface temperature fields associated with West African rainfall anomaly types. J Climate 9: 2935–2940

Geerts B, Dejene T (2005) Regional and diurnal variability of the vertical structure of precipitation systems in Africa based on spaceborne radar data. J Climate 18: 893–916

Halverson J, Rickenbach T, Roy B, Pierce H, Williams E (2002) Environmental characteristics of convective systems during TRMM-LBA. Mon Wea Rev 130: 1493–1509

Heymsfield GM, Geerts B, Tian L (2000) TRMM precipitation radar reflectivity profiles as compared with high-resolution airborne and ground-based radar measurements. J Appl Meteor 39: 2080–2102

Hirose M, Nakamura K (2004) Spatiotemporal variation of the vertical gradient of rainfall rate observed by the TRMM precipitation radar. J Climate 17: 3378–3397

Hirose M, Oki R, Shimizu S, Kachi M, Higashiuwatoko T (2007) Fine-scale diurnal rainfall statistics refined from 8 years. J Appl Meteor Climatol (Accepted)

Hobbs PV, Politovich MK, Radke IF (1980) The structures of summer convective clouds in eastern montana. 1. Natural clouds. J Appl Meteor 19: 645–663

Hodges KI, Thorncroft CD (1997) Distribution and statistics of African mesoscale convective weather systems based on the ISCCP Meteosat imagery. Mon Wea Rev 125: 2821–2837

Houze RA Jr (1997) Stratiform precipitation in regions of convection: a meteorological paradox? Bull Amer Meteor Soc 78: 2179–2196

Houze RA Jr, Betts AK (1981) Convection in GATE. Reviews Geophys Space Phys 19: 541–576

Iguchi T, Meneghini R (1994) Intercomparison of single-frequency methods for retrieving a vertical rain profile from airborne or spaceborne radar data. J Atmos Oceanic Technol 11: 1507–1516

Iguchi T, Kozu T, Meneghini R, Awaka J, Okamoto K (2000) Rain-profiling algorithm for the TRMM Precipitation Radar. J Appl Meteor 39: 2038–2052

Kalnay E, Kanamitsu M, Kistler R, Collins W, Deaven D, Gandin L, Iredell M, Saha S, White G, Woollen J, Zhu Y, Chelliah M, Ebisuzaki W, Higgins W, Janowiak J, Mo KC, Ropelewski C, Wang J, Leetmaa A, Reynolds R, Jenne R, Joseph D (1996) The NCEP/NCAR 40-year reanalysis project. Bull Amer Meteor Soc 77: 437–471

Kozu T, Kawanishi T, Kuroiwa H, Kojima M, Oikawa K, Kumagai H, Okamoto K, Okumua M, Nakatsuka H, Nishikawa K (2001) Development of precipitation radar onboard the Tropical Rainfall Measuring Mission (TRMM) satellite. IEEE T Geosci Remote 39L: 102–116

Kummerow C, Barnes W, Kozu K, Shiue J, Simpson J (1998) The Tropical Rainfall Measuring Mission (TRMM) sensor package. J Atmos Oceanic Technol 15: 809–817

Kummerow C, et al (2000) The status of the Tropical Rainfall Measuring Mission (TRMM) after two years in orbit. J Appl Meteor 39: 1965–1982

Laing AG, Fritsch JM (1997) The global population of mesoscale convective complexes. Quart J Roy Meteor Soc 123: 389–405

Lebel T, Diedhiou A, Laurent H (2003) Seasonal cycle and interannual variability of the Sahelian rainfall at hydrological scales. J Geophys Res-Atmospheres 108: Art. No. 8389

Lin JL, Mapes B, Zhang MH, Newman M (2004) Stratiform precipitation, vertical heating profiles, and the Madden-Julian oscillation. J Atmos Sci 61: 296–309

Mohr KI (2004) Interannual, monthly, and regional variability in the wet season diurnal cycle of precipitation in sub-Saharan Africa. J Climate 17: 2441–2453

Negri AJ, Bell TL, Xu L (2002) Sampling of the diurnal cycle of precipitation using TRMM. J Atmos Oceanic Technol 19: 1333–1344

Nesbitt SW, Zipser EJ (2003) The diurnal cycle of rainfall and convective intensity according to three years of TRMM measurements. J Climate 16: 1456–1475

Nicholson SE, Some B, McCollum J, Nelkin E, Klotter D, Berte Y, Diallo BM, Gaye I, Kpabeba G, Ndiaye O, Noukpozounkou JN, Tanu MM, Thiam A, Toure AA, Traore A (2003) Validation of TRMM and other rainfall estimates with a high-density gauge dataset for West Africa. Part I: validation of GPCC rainfall product and pre-TRMM satellite and blended products. J Appl Meteor 42: 1337–1354

Paeth H, Friederichs P (2004) Seasonality and time scales in the relationship between global SST and African rainfall. Clim Dynam 23: 815–837

Petersen WA, Rutledge SA (2001) Regional variability in tropical convection: observations from TRMM. J Climate 14: 3566–3586

Petersen WA, Fu R, Chen MX, Blakeslee R (2006) Intraseasonal forcing of convection and lightning activity in the southern Amazon as a function of cross-equatorial flow. J Climate 19: 3180–3196

Reed RJ (1977) Structure and properties of African wave disturbances as observed during phase III of GATE. Mon Wea Rev 105: 317–1977

Redelsperger JL, Diongue A, Diedhiou A, Ceron JP, Diop M, Gueremy JF, Lafore JP (2002) Multi-scale description of a Sahelian synoptic weather system representative of the West African monsoon. Quart J Roy Meteor Soc 128: 1229–1257

Rotunno R, Klemp JB, Weisman ML (1988) A theory for strong, long-lived squall lines. J Atmos Sci 45: 463–485

Roux F (1988) The West-African squall line observed on 23 June 1981 during COPT-81: Kinematics and thermodynamics of the convective region. J Atmos Sci 45(3): 406–426

Rowell DP, Milford JR (1993) Generation of African squall lines. J Climate 6: 1181–1193

Sauvageot H, Mesnard F, Tenorio RS (1999) The relation between the area-average rain rate and the rain cell size distribution parameters. J Atmos Sci 56: 57–70

Sealy A, Jenkins GS, Walford SC (2003) Seasonal/regional comparisons of rain rates and rain characteristics in West Africa using TRMM observations. J Geophys Res-Atmospheres 108 (D10): Art. No. 4306

Schumacher C, Houze RA Jr (2003) Stratiform rain in the tropics as seen by the TRMM Precipitation Radar. J Climate 16: 1739–1756

Schumacher C, Houze RA, Kraucunas I (2004) The tropical dynamical response to latent heating estimates derived from the TRMM precipitation radar. J Atmos Sci 61: 1341–1358

Schumacher C, Houze RA Jr (2006) Stratiform precipitation production over sub-Saharan Africa and the tropical east Atlantic as observed by TRMM. Quart J Roy Meteor Soc 132: 2235–2255

Simpson J, Adler RF, North GR (1988) A proposed Tropical Rainfall Measuring Mission (TRMM) satellite. Bull Amer Meteor Soc 69: 278–295

Steiner M, Houze RA Jr (1997) Sensitivity of the estimated monthly convective rain fraction to the choice of Z-R relation. J Appl Meteor 36: 452–462

Stith JL, Dye JE, Bansemer A, Heymsfield AJ, Grainger CA, Petersen WA, Cifelli R (2002) Microphysical observations of tropical clouds. J Appl Meteor 41: 97–117

Toracinta ER, Cecil DJ, Zipser EJ, Nesbitt SW (2002) Radar, passive microwave, and lightning characteristics of precipitating systems in the Tropics. Mon Wea Rev 130: 802–824

Weisman ML, Rotunno R (2004) A theory for strong long-lived squall lines revisited. J Atmos Sci 61: 361–382

Williams E, et al (2002) Contrasting convective regimes over the Amazon: Implications for cloud electrification. J Geophys Res-Atmospheres 107: D20 8082 (doi: 10.1029/2001JD000380)

Yuter SE, Houze RA (1995) 3-Dimensional kinematic and microphysical evolution of Florida cumulonimbus. Part 1: spatial-distribution of updrafts, downdrafts, and precipitation. Mon Wea Rev 123: 1921–1940

Authors' addresses: Jose D. Fuentes (e-mail: jf6s@virginia.edu), Teferi Dejene, Paolo D'Odorico, Department of Environmental Sciences, University of Virginia, 291 McCormick Road, Clark Hall, Charlottesville, VA 22904, USA; Bart Geerts, Department of Atmospheric Science, University of Wyoming, Laramie, WY 82071, USA; Everette Joseph, Department of Physics, Howard University, Washington, DC 20059, USA.